INTERNATIONAL SOCIETY FOR SOIL MECHANICS AND GEOTECHNICAL ENGINEERING

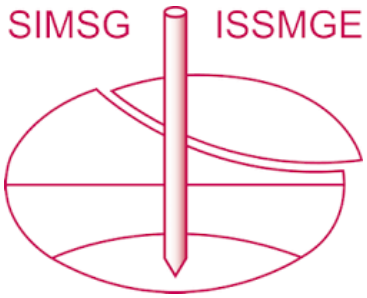

This paper was downloaded from the Online Library of the International Society for Soil Mechanics and Geotechnical Engineering (ISSMGE). The library is available here:

https://www.issmge.org/publications/online-library

This is an open-access database that archives thousands of papers published under the Auspices of the ISSMGE and maintained by the Innovation and Development Committee of ISSMGE.

The paper was published in the proceedings of the 10th European Conference on Numerical Methods in Geotechnical Engineering and was edited by Lidija Zdravkovic, Stavroula Kontoe, Aikaterini Tsiampousi and David Taborda. The conference was held from June 26th to June 28th 2023 at the Imperial College London, United Kingdom.

To see the complete list of papers in the proceedings visit the link below:

https://issmge.org/files/NUMGE2023-Preface.pdf

Proceedings 10th NUMGE 2023
10th European Conference on Numerical Methods in Geotechnical Engineering
Zdravkovic L, Kontoe S, Taborda DMG, Tsiampousi A (eds)

© Authors: All rights reserved, 2023
https://doi.org/10.53243/NUMGE2023-259

Performance of SANISAND-MS in modelling cyclic response of suction buckets in sand

A. Roy[1], H. Liu[2], A. Diambra[3], S.H. Chow[1], B. Bienen[4]

[1]*Department of Infrastructure Engineering, University of Melbourne, Australia*
[2]*Norwegian Geotechnical Institute, Oslo, Norway*
[3]*Department of Civil Engineering, University of Bristol, Bristol, UK*
[4]*Centre for Offshore Foundations, University of Western Australia, Perth, Australia*

ABSTRACT: This paper provides an assessment on the implementation and performance of the SANISAND-MS constitutive model in predicting the response of suction buckets under in-service operational loads. SANISAND-MS is a bounding surface plasticity model, enhanced with a memory surface (MS) to simulate the increasing sand stiffness and ratcheting under long-term drained cyclic loading. The paper begins with the calibration of the SANISAND-MS model parameters against a set of cyclic triaxial tests, involving a fine silica sand, performed at different densities and stress levels. The model is then implemented in the commercial finite element (FE) software ABAQUS. Aspects of the implementation, including the effect of model parameters and mesh size at critical locations for a boundary value problem of suction buckets, are examined in the paper. The model is then used to study in-service performance of a suction bucket under cyclic loading of different cyclic amplitudes in sand. The results are compared to those from experimental literature and insights are drawn from the numerical results. The study will benefit future FE implementation of sophisticated soil constitutive models.

Keywords: memory surface models; cyclic loading; sands; suction buckets; numerical modelling.

1 INTRODUCTION

Suction buckets are a foundation option for offshore wind turbines, and will experience several million load cycles during their operational lifetime (Bhattacharya et al., 2020) under the influence of wind and waves. Therefore, improving the geotechnical understanding of suction buckets under cyclic loads becomes of considerable importance. Tjelta (2015) provides an overview of the suction foundation technology and relative challenges. The majority of the research on suction buckets under in-service loads involve physical experiments. Numerical studies on suction buckets are limited (but include Cerfontaine et al., 2016), mainly because of non-avalibility of constitutive models suited for cyclic loading in libraries of commercial codes. With the recent developement of sophisticated constitutive models (Liu et al. 2019, Wichtmann et al. 2010), there is increasing interest to extend and explore their performances from element level to a boundary value problem.

This paper presents a qualitative assessment of the SANISAND-MS model perfomance in predicting the behaviour of suction buckets under in-service loads in Baskarp sand. Due to a lack of soil element test results on Baskarp sand, the model has been calibrated to four drained cyclic triaxial tests on UWA silica sand which has a similar grain size distribution as discussed later. The calibrated parameters are then used in a finite element (FE) analysis to capture the behaviour of two centrifuge tests on suction bucket foundations subjected to cyclic loading characterised by medium and high compressive mean loads respectively. The simulations were compared against reported experiments, which reveal valuable insights on the behaviour of the model and how the calibrated parameters perform when extrapolated from the cyclic triaxial loading conditions at element scale to boundary value problems.

2 METHODOLOGY

2.1 Soil model details

The numerical simulations were performed in the FE software ABAQUS using SANISAND-MS constitutive model (Liu et al. 2019). The SANISAND-MS model builds on a bounding surface plasticity framework (Dafalias and Manzari, 2004), but enhanced with an additional memory surface (MS) (initially proposed by Corti et al. 2016) to simulate the increasing sand stiffness and ratcheting behaviour observed under long-term drained cyclic loading. The model consists of the usual narrow conical yield surface that simultaneously

interacts with four other conical surfaces, namely the bounding surface, dilatancy surface, critical state surface and the memory surface. The model performance is state parameter dependent (ψ), which enables the simulation of various stress and density states using the same set of parameters.

Frictional material under cyclic loading undergoes cyclic shearing, leading to increased stiffness and changing dilation/contraction rate over several cycles under drained condition. This is tackled by a macroscopic introduction of the conical-shaped MS that serves to demarcate the region of non-virgin and virgin loading. The MS mainly supplements two model features, namely the plastic modulus (K_p) and the dilatancy. Contrary to the SANISAND04 version (Dafalias and Manzari, 2004), the current version incorporates an additional dependence of the MS on K_p using the expression:

$$K_p = \frac{2}{3} p \, \frac{b_0 \, (r^b - r) : n}{(r - r_{in}) : n} \, exp\left[\mu_0 \left(\frac{p}{p_{atm}}\right)^{0.5} \left(\frac{b^M}{b_{ref}}\right)^2\right] \quad (1)$$

where the term $(r^b - r) : n$ accounts for the distance between the current position of the yield surface and the bounding surface, b^M (= $(r^M - r) : n$) accounts for the distance between the current position of the yield surface and the memory surface, μ_0 is a model parameter controlling the intensity of b^M in the expression and b_0 is a factor accounting for the effect of void ratio and mean stress. An increase in MS size is promoted by contractive deformations through a fabric reinforcement, while a shrinkage in MS size leading to loss of memory is promoted through dilative deformations (Liu et al. 2019). The change in MS size is implemented as:

$$\mathrm{d}m^M = \sqrt{\frac{3}{2}} \mathrm{d}\alpha^M : n - \frac{m^M}{\zeta} f_{shr} \langle -d^p_{vol} \rangle \quad (2)$$

where the f_{shr} is a geometric factor, d^p_{vol} is the incremental plastic volumetric strain, α^M is the back-stress tensor of the MS, m^M is the current size of the MS and ζ is a model parameter. The kinematic hardening is incorporated by a parallel translation of the MS along the direction of movement of the yield surface as:

$$\mathrm{d}\alpha^M = \frac{2}{3} \langle L^M \rangle h^M \left(r^b_\theta - r^M\right) \quad (3)$$

where h^M is the hardening modulus for the MS and L^M is the loading index.

2.2 FE model details and methodology

The suction bucket problem was modelled through a series of wished-in-place axisymmetric analyses using a structured mesh (Figure 1) composed of linear quadrilateral elements (CAX4). The analyses considered a bucket with a diameter (D) of 8 m and a skirt length (L) of 4 m (aspect ratio L/D = 1:2) and thickness (t) of 50 mm. This is in the range of 0.5 – 1.0 for usual bucket aspect ratios installed in the North sea. The relative density (R_D) of the sand was chosen as 95%. The bucket size and sand density were selected to replicate the centrifuge tests by Bienen et al. (2018a), which serve as the validation database for this numerical study. The coefficient of earth pressure (K_0) for the soil was taken as 0.5.

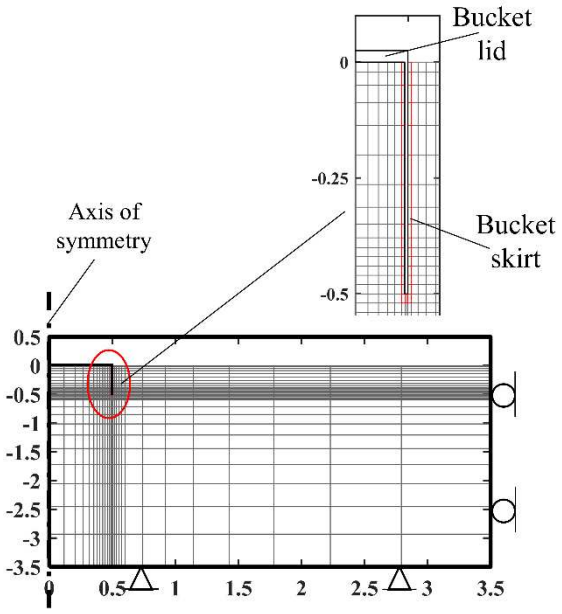

Figure 1: Representative mesh used in the simulations

The bucket was modelled as fully rigid, with the bucket centre being taken as the reference point for the application of displacements. The bottom and lateral boundaries of the domain were kept at 3.5D from the centre of the bucket. Nodes on the bottom boundary were fully restrained, and only lateral restraint was imposed for nodes on the side boundaries. Minimum size of the element for the soil within the bucket were maintained at 0.02D to capture the settlement characteristics accurately.

On drained compression, a suction bucket mobilises resistance in shearing along its skirts and in bearing as the lid and skirt tip push against the soil directly underneath. To accurately capture the strain localisation around the skirts, the thickness of the element around the skirt ideally needs to be of the order of the shear band thickness (~ 10D_{50}). However, modelling such a thin layer would be numerically prohibitive. So, from practical considerations, the element thickness around the skirt has been kept equal to the skirt thickness of 50 mm in the analysis. Implications will be discussed in the subsequent sections.

Model buckets used in the experiments were made out of anodised aluminium, for which Whyte (2019) reported an interface angle (δ_p) between 20° and 22°. A reasonable estimation of δ_p can be obtained through a drained uplift test on a suction bucket, wherein the soil does not plug within the bucket. Bienen et al. (2018a)

reported an uplift stress of 15 kPa on drained pullout test of a suction bucket in dense Baskarp sand, which corresponded to an interface friction angle of 21° (for a modest $K_0 = 0.5$). The present simulations have adopted soil-skirt interface δ_p of 15° (such that the interface coefficient was 0.25), which is slightly lower than the experimentally observed value to reduce numerical convergence issues.

PIV tests in very dense sand (Ragni et al. 2020) have shown that soil around the interface up to an influence zone of ~1t undergoes dilation by an average margin of 10.9% during suction installation under seepage flow gradients. Koteras and Ibsen (2019) reported a R_D reduction of ~30% in dense sands after suction installation, computed as per CPT tip reduction values within the soil plug before and after installation. This contrasts with the findings in Stapelfeldt et al.(2020), who observed a marginal effect of suction installation on the soil plug. In the present analysis, the potential installation disturbances have been macroscopically accounted for by defining a 50 mm layer of reduced stiffness on either side of the skirt (red layer in Figure 1) using a lower stiffness parameter ($G_0 = 95$ MPa instead of 135 MPa, more details in Section 4).

3 CALIBRATION OF MODEL PARAMETERS

This section reports the SANISAND-MS model parameter calibration based on cyclic triaxial tests on UWA silica sand. Table 1 lists the silica sand properties, along with that of Baskarp sand reported in the validation centrifuge studies (Bienen et al. 2018a).

Table 1: Physical properties of UWA and Baskarp sands

Soil Properties	UWA silica sand[a]	Baskarp sand[b]
D_{60} (mm)	0.2	0.17
D_{50} (mm)	0.19	0.15
D_{10} (mm)	0.119	0.1
U	1.68	1.70
e_{max}	0.789	0.86
e_{min}	0.512	0.57

[a] From Roy et al. (2021); [b] From Bienen et al. (2018a)

The SANISAND-MS model has a total of 17 model parameters. 14 of them, that were previously introduced in the SANISAND04 (Dafalias and Manzari, 2004) version to capture the monotonic behaviour, have been kept identical to the ones calibrated and reported for monotonic TXC tests on UWA Silica sand (Roy et al. 2021). The 3 cyclic parameters are then calibrated by optimising the model predicted accumulated cyclic strains against those measured from the four element tests. These element tests were performed on a set of water-pluviated anisotropically consolidated ($K_0 = \sigma_h' / \sigma_v' = 0.5$) samples on UWA sand at a frequency of 0.5 Hz. Table 2 lists the test program involving medium-dense (R_D ~ 60%) and dense samples (R_D = 88%) across a wide range of initial mean effective stress (p'_{in} = 60 – 1500 kPa). The tests were conducted at an initial deviatoric stress ratio ($\eta_{in} = q_{in} / p'_{in}$) of 0.75, with a cyclic stress ratio ($\eta_{cy} = q_{cy} / p'_{in}$) being maintained at 0.2. Table 3 presents the calibrated model parameters.

Table 2: Cyclic triaxial test details on UWA silica sand

ID	R_D (%)	p'_{in} (kPa)	q_{in} (kPa)	$\eta_{cy} = q_{cy} / p'_{in}$	q_{cy} (kPa)
1	60	200	150	0.2	40
2	88.1	200	150	0.2	40
3	50.9	1500	1125	0.2	300
4	57.1	80	60	0.2	16

Figure 2 compares the accumulated strain norm ($\varepsilon^{acc} = \sqrt{(\varepsilon_a^{acc})^2 + 2(\varepsilon_r^{acc})^2}$, where the subscripts, 'a' and 'r' stand for axial and radial components respectively) simulated using the calibrated model parameters against those from the experiments. The measured responses show that ε^{acc} increases with an increase in p'_{in} and a reduction in R_D. This trend is satisfactory captured in the simulated responses for all four tests. It is also found that the measured ε^{acc} accumulates sharply in Test 2 and 4 after 1000 cycles, suggesting that possible inhomogeneity may have developed in the samples with prolonged shearing. Hence the parameters were optimised to obtain a proper fit for the first 1000 cycles across all the tests.

Table 3: SANISAND-MS parameters for UWA silica sand

Parameters	Symbol	Value
Elastic properties	G_0	135
	ν	0.14*
Parameters controlling the slope and intercept of critical state line	e_o	0.812
	λ	0.0189
	ξ	0.7
	M	1.296
	c_1	0.7
Yield surface size	m	0.05*
Parameter for plastic potential gradient	c_2	0.78*
Parameters influencing plastic modulus	h_0	7.5
	c_h	1.01
	n^b	2.0
Parameters influencing dilatancy	A_0	0.84
	n^d	3.4 (2.8)
Memory surface parameters	μ_0	85
	ζ	0.001
	β	1.0

*Assumed

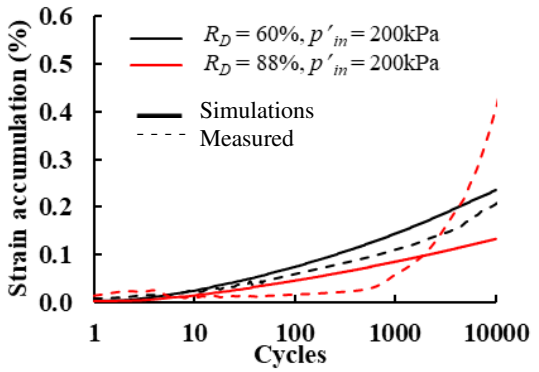

(a)

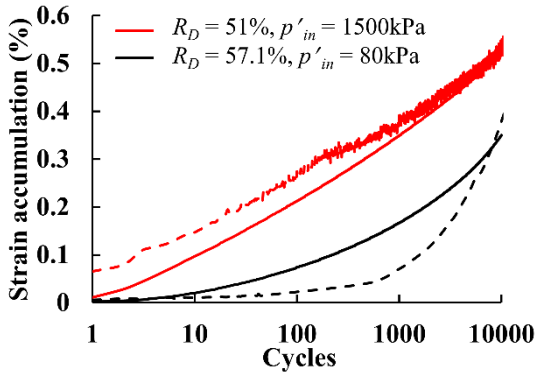

(b)

Figure 2: Simulated and measured accumulated strain norm for (a) Test 1 and Test 2, and (b) Test 3 and Test 4

4 VALIDATION AGAINST CENTRIFUGE TESTS

The performance of the calibrated model has been validated against two drained centrifuge tests on suction buckets reported in Bienen et al. (2018b) on Baskarp sand. The particle size distribution and soil properties for Baskarp sand (Table 1) are close to that of UWA Silica sand, hence it is expected that the cyclic behaviour of the two sands would be relatively similar. The centrifuge tests in saturated Baskarp sand involved R_D ~98% at 100g using bucket models of diameter of 80 mm, length of 40 mm and a thickness of 0.5 mm (representing an equivalent prototype bucket having D = 8 m, L = 4 m and skirt thickness, t = 50 mm in the numerical model).

The respective loading histories for the two tests but were chosen to represent a: a) state of low mean stress (σ_m = 60 kPa) on the leeward side, and b) state of higher σ_m = 550 kPa on the windward side respectively. These two tests in Bienen et al., (2018b), refererred to as Test 6_5 and Test 4_3, were performed on multi-parcel cyclic loads. In the present simulations, only the first 2 parcels and 3 parcels from Test 6_5 and Test 4_3 respectively were selected as they were effectively drained in the experiments. The remaining parcels were not simulated as they produced partially drained response which is beyond the scope of current numerical study. The cyclic amplitudes (σ_{cy}) for parcels 1 and 2 were 16 kPa and 40 kPa for the test with σ_m = 60 kPa representative of moderately calm sea states, whereas σ_{cy} were 77 kPa, 162 kPa and 325 kPa for the test with σ_m = 550 kPa representative of storm conditions as assumed in the medium scale field tests discussed in Kelly et al. (2006). As previously mentioned, a weak layer on either side of the skirt has been introduced by using a G_0 of 95 MPa (while keeping the other soil model parameters unchanged). This approach is similar to the one followed for monopile modelling in Liu et al. (2020).

The simulated and measured normalised accumulated settlement (δ_{acc}/L) for the two tests are compared in Figures 3 and 4. For the test with with σ_m = 60 kPa, the simulations produce a δ_{acc} of 0.0022L (in grey) and 0.0015L (in blue) over 1000 cycles and 100 cycles respectively (Figure 3). When compared against the centrifuge results, the simulated δ_{acc}/L is within 10% for the 1st load parcel, but 50% lower than those observed in the 2nd load parcel (more discussion later).

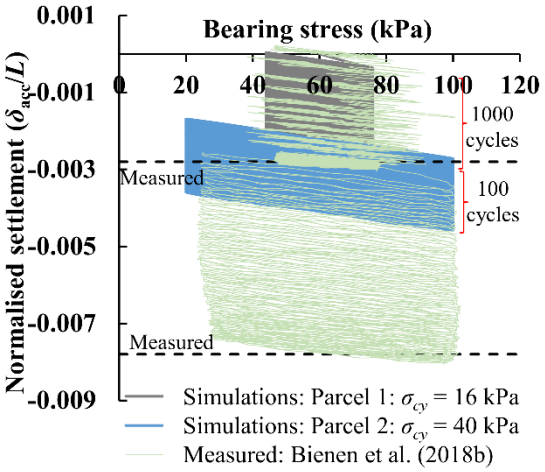

Figure 3:Comparsion between the simulations and the experiments for the test having σ_m = 60 kPa

For test with σ_m = 550 kPa, the simulations produce a settlement of 0.002L (in grey), 0.005L (in blue) and 0.008L (in red) at the end of the three parcels having 10 cycles each of σ_{cy} of 77 kPa, 162 kPa and 325 kPa respectively (Figure 4). As compared to the simulations with σ_m = 60 kPa, the values of σ_{cy} and σ_m for this test being higher, the settlement accumulation loops are gradually more non-symmetrical for the bucket, with more asymmetries being observed at the higher cyclic load than at the lower load. The simulations, when compared with the centrifuge results, are within 10% for the 1st and 2nd load parcel, but 50% lower those observed in the 3rd load parcel.

Overall, the simulated results from the tests show that the SANISAND-MS model can satisfactorily capture the trends for the tests at low cyclic ratios (η_{cy} < 0.3) but underpredicts δ_{acc} for load packages having η_{cy} > 0.6. It needs to be recalled that the parameters used to replicate the suction bucket simulations were obtained from element tests subjected to η_{cy} = 0.2, hence more element

testing data at η_{cy} > 0.3 would be required to provide more insights on the underprediction at higher η_{cy}.

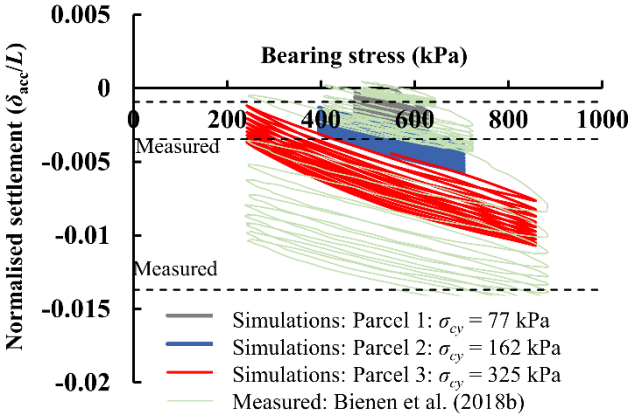

Figure 4: Comparsion between the simulations and the experiments for the test having σ_m = 550 kPa

To investigate the systematic underprediction further, two additional numerical simulations were undertaken for the case with R_D = 98% having a 2-parcel load combination as in Figure 3. Firstly, an attempt was made to investigate the effect of mesh dependence on the problem, wherein the thickness of the element along the skirt was reduced from 50 mm to 30 mm in an attempt to better capture the skirt friction contribution and the stress gradients around the skirt tip. Ideally, the thickness should have been taken in the order of shear band thickness (~10D_{50}) expected in the mechanism. For prototype-sized bucket foundation having 50 mm thick skirt, the expected shear band thickness would be approximately 2 mm or ~0.04t (or even smaller), whereas for the centrifuge test models, this would be ~4t. The simulations used a thickness of 50 mm (=1t), which lies between the expected limits. Figure 5 reports the results from an additional simulation, that used a thinner element of 30 mm (0.6t) to resimulate the bucket model with the load parcel as in Figure 3. The results (Figure 5) show that using a thinner element increases the δ_{acc}/L values in parcel 1 over 1000 cycles by 18% and a further by 22% in parcel 2 over 100 cycles. This shows the importance of selecting appropriate mesh size based on the expected failure mechanism when simulating load-controlled shearing-dominated problems. It also needs to be mentioned that, if compared to the analysis with the coarser mesh, these simulations with a finer mesh are twice more computationally expensive on a Intel(R) Core(TM) i7-8550U 1.8GHzCPU processor.

The higher δ_{acc} measured in the centrifuge tests also suggests that there is a larger contractancy below the bucket under cyclic loads than what is being captured in the FE simulations. This could potentially be rectified by adjusting selected SANISAND-MS model parameters (Table 3). For instance, the value of μ_0 could be lowered so that the plastic modulus K_p in the governing expressions is decreased, however this alone would not suffice to reconcile the differences between the simulations and the experiments. The simulations can be improved significantly by opting for a lower n^d value. For dense sand, ψ being negative (same for Baskarp sand in the experiments), the dilatancy surface lies inside the critical surface; using a smaller n^d shifts the dilatancy surface closer to the critical surface and increases the distance between the yield and the dilatancy surface under compressive states, thus promoting more compression in the model responses. The results from such an exercise using n^d = 2.8, with a mesh having an element size of 50 mm (in Figure 6), shows that the revised simulations produce settlements that are 40% higher over the two load parcels than those with n^d = 3.4 and better match the reported experiments. Considering that a thinner element along the skirt (i.e. 30 mm) would have produced a δ_{acc}/L value ~20% higher, this simulation exercise would have produced results much closer to the experimental results.

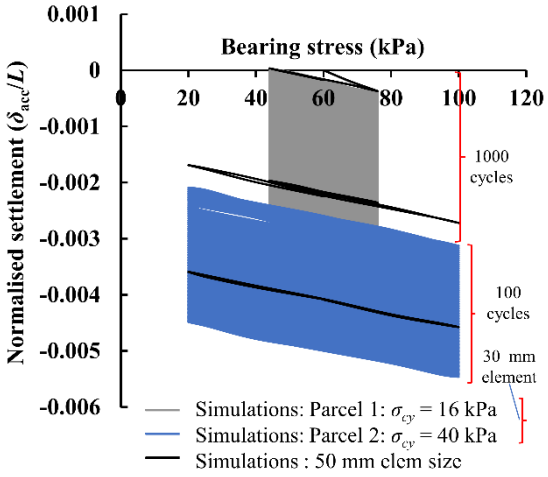

Figure 5: Effect of element size around the bucket skirt on the simulations for the test having σ_m = 60 kPa

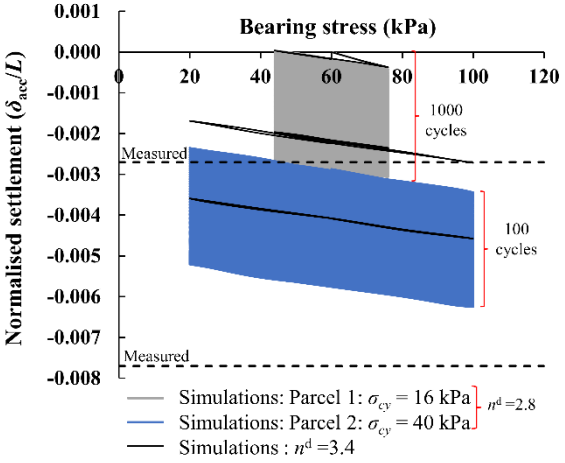

Figure 6: Effect of parameter n_d on the numerical simulations for test having σ_m = 60 kPa

This exercise highlights a possible challenge in calibration, wherein calibrated monotonic parameters, especially relating to dilatancy surface or stiffness, may not necessary hold for cyclic response. Similar finding was also reported by Jostad et al. (2020) for the SANISAND04 model, where the monotonic parameter

set performed poorly when extended to capture cyclic responses. Based on this evidence, proportional adjustment of monotonic dilatancy parameter n^d appears justifiable in this study. However, the effect of adjusting n^d for boundary value problems involving different stress paths needs further exploration.

5 CONCLUSIONS

This paper has investigated the performance of the SANISAND-MS model in modelling cyclic responses of suction buckets in dense sand. The model was initially calibrated against four cyclic triaxial drained tests across a range of initial mean effective stress, followed by subsequent FE simulations of a multi-parcel cyclic loading on a suction bucket. The key findings are:

- The constitutive model satisfactorily captures the element level responses of increasing accumulated strain norms with an increase in average mean stress and a reduction in sand relative density.
- The same constitutive parameters calibrated from the triaxial element tests, when applied to simulate the multi parcel cyclic loading on suction buckets at two different average cyclic stress levels (60kPa and 550 kPa), were able to capture the accumulated settlements for load parcels having cyclic stress ratios below 0.3, but underestimated settlements for parcels having cyclic stress ratios greater than 0.3. This suggests that, for satisfactory performance, the element tests for calibration need to consider the cyclic load and amplitude levels expected in the field.
- Retrospective analysis proved that ~18% of the underestimation in accumulated settlements could be attributed to the choice of the minimum element size around the bucket skirt.
- Corrective attempts by adopting a lower dilatancy stress ratio could reduce the mismatch between the simulations and the centrifuge responses. Overall, checking model performance, both against element tests and relevant boundary value problems, appears to be more of a judicious way for calibration.

6 ACKNOWLEDGEMENTS

The first author was supported by the Australian Research Council Discovery Grant Scheme (project number DP190100914).

7 REFERENCES

Bhattacharya, S., Nikitas, G., Aleem, M., Cui, L., Wang, Y., Jalbi, S., Hilton, J. 2020. Challenges in the Design and Construction of Offshore Wind Turbine Foundations Including Sites in Seismic Areas. *Advances in Offshore Geotechnics: Proceedings*, ISOG2019 (Eds. Halder, S., Patra, S., Ghanekar, R.),121-160. Springer, Singapore.

Bienen, B., Klinkvort, R.T., O'Loughlin, C.D., Zhu, F., Byrne, B.W. 2018a. Suction caissons in dense sand, part I: Installation, limiting capacity and drainage, *Géotechnique* 68(11), 937–952.

Bienen, B., Klinkvort, R.T., O'Loughlin, C.D., Zhu, F., Byrne, B.W. 2018b. Suction caissons in dense sand, part II: vertical cyclic loading into tension, *Géotechnique* 68(11), 953–967.

Cerfontaine, B., Collin, F., Charlier, R. 2016. Numerical modelling of transient cyclic vertical loading of suction caissons in sand, *Géotechnique* 66(2), 121-136.

Corti, R., Diambra, A., Wood, D.M., Escribano, D.E., Nash, D.F.T. 2016. Memory surface hardening model for granular soils under repeated loading conditions. *J. Eng. Mechanics* 142(12), 04016102.

Dafalias, Y.F., Manzari, M.T. 2004. Simple Plasticity Sand Model Accounting for Fabric Change Effects, *J. Eng. Mechanics* 130(6), 622–634.

Jostad, H.P., Dahl, B.M., Page, A., Sivasithamparan, N., Sturm, H. 2020. Evaluation of soil models for improved design of offshore wind turbine foundations in dense sand, *Géotechnique* 70(8), 682–699.

Koteras, A., Ibsen, L. 2019. Medium-scale Laboratory Model of Mono-bucket Foundation for Installation Tests in Sand, *Canadian Geotechnical Journal* 56(8),1142–1153.

Liu, H.Y., Abell, J.A., Diambra, A., Pisano, F. 2019. Modelling the cyclic ratcheting of sands through memory-enhanced bounding surface plasticity, *Geotechnique* 69(9), 783–800.

Liu, H.Y., Kementzetzidis, E., Abell, J.A., Pisano, F. 2020. From cyclic sand ratcheting to tilt accumulation of offshore monopiles: 3D FE modelling using SANISAND-MS, *Geotechnique* 72(9), 753-768.

Ragni, R., Bienen, B , Stanier,S., O'Loughlin, C.D., Cassidy, M. 2020. Observations during suction bucket installation in sand, *International Journal of Physical Modelling in Geotechnics* 20(3),132–149.

Roy, A., Chow, S.H., O'Loughlin, C.D., Randolph, M.F., Whyte, S. 2021. Use of bounding surface model in predicting element tests and capacity in boundary value problems, *Canadian Geotechnical Journal* 58(6), 782-799.

Stapelfeldt, M., Bienen, B., Grabe, J. 2020. The influence of the drainage regime on the installation and the response to vertical cyclic loading of suction caissons in dense sand, *Ocean Engineering 215*.

Tjelta, T. 2015. The suction foundation technology. *Frontiers in Offshore Geotechnics* III, *Proceedings*, ISFOG'2015, (Eds. Meyer,V.), 85-93. Taylor & Francis Group, London.

Wichtmann, T., Niemunis, A., Triantafyllidis, T. 2010. Strain accumulation in sand due to drained cyclic loading: On the effect of monotonic and cyclic preloading (Miner's rule), *Soil Dynamics and Earthquake Engineering* 30(8), 736–745.

Whyte, S.A. 2019. *Development, Implementation, Calibration and use of Practical Constitutive Models in Finite Element Analysis of Offshore Foundations*. PhD Thesis, University of Oxford